

# On the Boolean model of Wiener sausages

Rostislav Cerny, Stefan Funken und Evgueni Spodarev

Preprint Series: 2006-06



Fakultät für Mathematik und Wirtschaftswissenschaften  
UNIVERSITÄT ULM

# On the Boolean model of Wiener sausages

Rostislav Černý, Stefan Funken und Evgueni Spodarev

Preprint Series: 2006-06



Fakultät für Mathematik und Wirtschaftswissenschaften  
UNIVERSITÄT ULM

# On the Boolean model of Wiener sausages

Rostislav Černý\*, Stefan Funken†, Evgueni Spodarev†

October 3, 2006

## Abstract

The Boolean model of Wiener sausages is a random closed set that can be thought of as a random collection of parallel neighborhoods of independent Wiener paths in space. It describes e.g. the target detection area of a network of sensors moving according to the Brownian dynamics whose initial locations are chosen in the medium at random. In the paper, the capacity functional of this Boolean model is given. Moreover, the one- and two-point coverage probabilities as well as the contact distribution function and the specific surface area are studied. In  $\mathbb{R}^2$  and  $\mathbb{R}^3$ , the one- and two-point coverage probabilities are calculated numerically by Monte Carlo simulations and as a solution of the heat conduction problem. The corresponding approximation formulae are given and the error of approximation is analyzed.

**Keywords:** Wiener sausage, Boolean model, sensor network, capacity, volume fraction, specific surface area, covariance function, contact distribution function, approximation, heat conduction problem, finite element method, Monte Carlo simulations, stochastic geometry

**AMS Subject Classification 2000:** Primary 60D05, 60J65;  
Secondary 65C05, 65M60

## 1 Introduction

A parallel neighborhood of a path of the Brownian motion is named after Norbert Wiener a *Wiener sausage*. This random closed set is used in physics, chemistry, biology and telecommunication to model various phenomena; cf. references in [23]. More complicated random closed sets can be constructed on its basis using the paradigm of *germ-grain models*. For that, a number

---

\*Charles University, Faculty of Mathematics and Physics, Sokolská 83, 18675 Praha 8, Czech Republic, Email: rostislav.cerny@mediaresearch.cz

†Faculty of Mathematics and Economics, University of Ulm, Helmholtzstr. 18, D-89069 Ulm, FRG, Email: {stefan.funken, evgueni.spodarev}@uni-ulm.de

of random locations in space called *germs* is supplied with random *grains* placed in these locations.

A germ–grain model with the spatially homogeneous Poisson point process of germs and independent identically distributed grains is a *Boolean model*. It is distinguished by the structural simplicity and the availability of analytical formulae for its characteristics; cf. e.g. [20]. Boolean models with convex, polyconvex or smooth grains appear naturally in many applications in materials science, biology and medicine; cf. e.g. [15]. For this reason, most applied papers deal with these very well studied classes of primary grains. Extending the class of possible grains to fractal sets such as Wiener sausages and providing analytical formulae for the new type of grains would give practitioners more flexibility in modelling rough geometric structures.

Boolean models of Wiener sausages appear in connection with sensor networks; cf. e.g. [17] and [11]. Imagine that sensors scattered initially at random in a non-transparent medium start moving according to the Brownian dynamics. Each sensor can detect a target within a range  $r > 0$ . The target detection area of such sensor network up to time  $T > 0$  forms a Boolean model with the Wiener sausage of radius  $r$  as a primary grain. The probability of target detection (also known as the *one–point coverage probability* or *volume fraction* of the Boolean model) in three dimensions is given in [11].

In this paper, we deal mainly with the *two–point coverage probabilities* of the Boolean model of Wiener sausages that are often called the *covariance function*. We give approximation formulae for the covariance function in two and three dimensions based on Monte Carlo simulations and numerical solutions of the heat conduction equation.

In Section 2, preliminaries on Wiener sausages are given. Section 3 deals with the capacity functional of the Boolean model of Wiener sausages connecting it with the initial and boundary value problems for the heat equation. A general representation of the volume fraction, the covariance function and the contact distribution function as values of the capacity functional on particular test sets follows easily. This representation involves an integral of the solution of the heat conduction problem in some region. For the covariance function, this is an exterior of the union of two (possibly overlapping) spheres. If these spheres coincide an explicit analytical solution can be given in any dimension. Nevertheless, in all dimensions excepting three this formula can not be used in practice since it involves integrals of a combination of Bessel functions. Moreover, in general case the corresponding analytical expression is still unknown and has to be assessed numerically. In Section 3.3, a formula for the specific surface area of the Boolean model of Wiener sausages is given. The numerical analysis of the covariance function in two and three dimensions is performed in Section 4 by means of finite element methods and by simulation (Sections 4.1 and 4.3, respectively). Simple approximation formulae are provided and the error of approximation is dis-

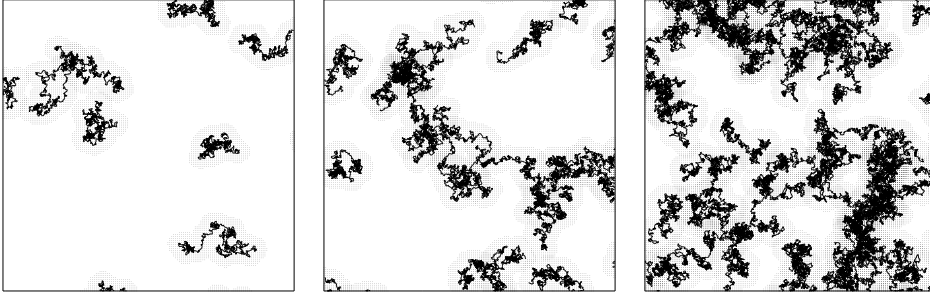


Figure 1: Three realizations of Boolean models of Wiener sausages for  $T = 10$  and  $r = 1$ . The intensity  $\lambda$  is chosen to fit volume fractions 0.25, 0.5 and 0.75, respectively.

cussed. Results of different computation methods are compared in Section 4.4. We conclude with a brief discussion of open problems.

## 2 Preliminaries

Let  $A \oplus B$  be the pointwise sum of two sets  $A$  and  $B$  in  $\mathbb{R}^d$ . For the ball  $B = B(o, r)$  of radius  $r \geq 0$  in  $\mathbb{R}^d$  centered at the origin, the set  $A_r = A \oplus B(o, r)$  is called the  $r$ -parallel neighborhood of  $A$ . The operation  $A \mapsto A_r$  is known as *dilation*. Let us write  $V_d(A)$  for the volume of a Borel set  $A \subset \mathbb{R}^d$ . For any set  $A$ , denote  $\check{A} = -A$ . Let  $\omega_d = \pi^{d/2}/\Gamma(1 + d/2)$  be the volume of the unit ball in  $d$  dimensions.

Let  $\{B^x(t), t \geq 0\}$  be the  $d$ -dimensional Brownian motion in  $\mathbb{R}^d$  with variance  $\sigma^2 > 0$  starting at  $B^x(0) = x \in \mathbb{R}^d$ . Throughout the paper, we assume that  $d \geq 2$ . Given a radius  $r > 0$  and a time  $T > 0$  we set

$$S_{r,T}^x = \{B^x(t) : 0 \leq t \leq T\} \oplus B(o, r). \quad (2.1)$$

$S_{r,T}^x$  is called the *Wiener sausage*; cf. e.g. [22], p. 64. It is a random compact set (in the sense of Matheron, see [14]). We shall write only  $S_{r,T}$  for  $S_{r,T}^o$  if the Brownian motion starts at the origin. It is known that all moments of the volume  $V_d(S_{r,T})$  are finite, see [21].

## 3 Boolean model of Wiener sausages

Assume  $\varphi = \{x_n\}_{n=1}^\infty$  to be a stationary Poisson point process in  $\mathbb{R}^d$  with intensity  $\lambda > 0$  (see e.g. [20] for more details). Consider an independent identically distributed collection of Wiener sausages  $\{(S_{r,T})_n\}_{n=1}^\infty$  (each starting at the origin) which are independent of the process  $\varphi$ . Introduce the *Boolean*

model  $\Xi$  of Wiener sausages by putting

$$\Xi = \bigcup_{n=1}^{\infty} (x_n + (S_{r,T})_n). \quad (3.1)$$

Since  $\mathbb{E} V_d(S_{r,T} \oplus B(o, r')) = \mathbb{E} V_d(S_{r+r',T}) < \infty$  for all  $r' > 0$ ,  $\Xi$  is a random closed set (see [20]). The isotropy of  $S_{r,T}$  and stationarity of  $\varphi$  imply that  $\Xi$  is stationary and isotropic. It means that the probability distribution of  $\Xi$  is invariant with respect to rigid motions.

### 3.1 Capacity functional, volume fraction and covariance function

The *capacity functional*  $T_{\Xi}(C) = P(\Xi \cap C \neq \emptyset)$  for all compact  $C \subset \mathbb{R}^d$  plays the same role in the theory of random sets as the distribution function of random variables in the classical probability theory. Namely, it defines the distribution law of  $\Xi$  uniquely. It is known that the capacity functional of the Boolean model is given by

$$T_{\Xi}(C) = 1 - e^{-\lambda \mathbb{E} V_d(S_{r,T} \oplus \check{C})} \quad (3.2)$$

for all compact  $C$ ; cf. [20].

Following [18], we can compute the expected volume of  $S_{r,T} \oplus \check{C}$  using Fubini's theorem as

$$\mathbb{E} V_d(S_{r,T} \oplus \check{C}) = \int_{\mathbb{R}^d} P(x \in S_{r,T} \oplus \check{C}) dx = \int_{\mathbb{R}^d} P\left(\tau_{C \oplus B(o,r)}^x \leq T\right) dx, \quad (3.3)$$

where  $\tau_A^x = \inf\{s \geq 0 : B^x(s) \in A\}$  is the first hitting time of a Borel set  $A$  for the Brownian motion starting at  $x \in \mathbb{R}^d$ . Introduce the notation  $u(t, x) = P\left(\tau_{C \oplus B(o,r)}^x \leq t\right)$ ,  $x \in \mathbb{R}^d$ ,  $t \geq 0$ . Kolmogorov and Leontovich [12], Hunt [10] and Doob [6] showed that  $u(t, x)$  is the unique bounded solution to the following heat conduction problem:

$$\begin{aligned} \frac{\partial u}{\partial t} &= \frac{\sigma^2}{2} \Delta u, & t > 0, x \in \mathbb{R}^d \setminus (C \oplus B(o, r)), \\ u(0, x) &= 0, & x \in \mathbb{R}^d \setminus (C \oplus B(o, r)), \\ u(t, x) &= 1, & t \geq 0, \text{ for all regular } x \in \partial(C \oplus B(o, r)), \end{aligned} \quad (3.4)$$

i.e. points  $x$  such that

$$P\left(\tau_{C \oplus B(o,r)}^x = 0\right) = 1. \quad (3.5)$$

Notice that all points of  $\partial(C \oplus B(o, r))$  are regular for almost all  $r > 0$  at least in dimensions two and three. Indeed, it is known that the probability

(3.5) can be either zero or one. Assuming that it is zero we arrive at a contradiction with the fact that  $\partial(C \oplus B(o, r))$  is a  $(d - 1)$ -dimensional Lipschitz manifold for almost all  $r > 0$  if  $d = 2$  or  $d = 3$ ; cf. [7].

For arbitrary compact sets  $C$  the problem (3.4) has to be solved by numerical methods. In some special cases (for instance, if  $C = \{o\}$ ) an analytical solution is given in [2]. This is the expected volume of the Wiener sausage:

$$\begin{aligned} \mathbb{E} V_d(S_{r,t}) &= \omega_d r^d + \frac{d(d-2)}{2} \omega_d \sigma^2 r^{d-2} t \\ &+ \frac{4d \omega_d r^d}{\pi^2} \int_0^\infty \frac{1 - e^{-\frac{\sigma^2 y^2 t}{2r^2}}}{y^3 (J_\nu^2(y) + Y_\nu^2(y))} dy, \quad d \geq 2, \end{aligned} \quad (3.6)$$

where  $J_\nu$  and  $Y_\nu$  are Bessel functions of the first and second kind of order  $\nu = (d - 2)/2$ . In three dimensions, this formula simplifies to

$$\mathbb{E} V_3(S_{r,t}) = \frac{4}{3} \pi r^3 + 4\sigma r^2 \sqrt{2\pi t} + 2\pi \sigma^2 r t, \quad (3.7)$$

compare [18].

The *volume fraction*  $p_\Xi$  of the Boolean model  $\Xi$  defined by

$$p_\Xi = \mathbb{P}(o \in \Xi) = \mathbb{E} V_d(\Xi \cap [0, 1]^d)$$

is just the one-point coverage probability of  $\Xi$ . It follows from relations  $p_\Xi = T_\Xi(\{o\})$ , (3.2) and (3.6) that

$$p_\Xi = 1 - e^{-\lambda \left( \omega_d r^d + \frac{d(d-2)}{2} \omega_d \sigma^2 r^{d-2} T + \frac{4d \omega_d r^d}{\pi^2} \int_0^\infty \frac{1 - e^{-\frac{\sigma^2 y^2 T}{2r^2}}}{y^3 (J_\nu^2(y) + Y_\nu^2(y))} dy \right)}. \quad (3.8)$$

For  $d = 3$  this formula can be found in [11].

The *covariance function* of the isotropic Boolean model  $\Xi$  can be introduced by

$$C_\Xi(h) = \mathbb{P}(o, h \cdot u \in \Xi), \quad (3.9)$$

where  $u$  is an arbitrary unit vector in  $\mathbb{R}^d$  and  $h \geq 0$ ; see [20] and [15]. It follows from (3.2) and the formula of total probability that

$$C_\Xi(h) = 2p_\Xi - T_\Xi(\{o, h \cdot u\}) = 2p_\Xi - 1 + e^{-\lambda \mathbb{E} V_d(S_{r,T} \cup (S_{r,T} + h \cdot u))}. \quad (3.10)$$

It follows from relations (3.2) and (3.3) that the mean volume

$$\mathbb{E} V_d(S_{r,T} \cup (S_{r,T} + h \cdot u)) = \int_{\mathbb{R}^d} \mathbb{P} \left( \tau_{B(o,r) \cup B(h \cdot u, r)}^x \leq T \right) dx \quad (3.11)$$

in formula (3.10) can be computed by integrating the solution of the heat conduction problem (3.4) where

$$C \oplus B(r, o) = \{o, h \cdot u\} \oplus B(o, r) = B(o, r) \cup B(h \cdot u, r). \quad (3.12)$$

The mean volume in (3.11) is related to the *covariogram*

$$C_{S_{r,T}}(h) = \mathbb{E} V_d(S_{r,T} \cap (S_{r,T} + h \cdot u))$$

of the Wiener sausage  $S_{r,T}$  by

$$\mathbb{E} V_d(S_{r,T} \cup (S_{r,T} + h \cdot u)) = 2 \mathbb{E} V_d(S_{r,T}) - \mathbb{E} V_d(S_{r,T} \cap (S_{r,T} + h \cdot u)) \quad (3.13)$$

where  $\mathbb{E} V_d(S_{r,T})$  is given in (3.6).

### 3.2 Contact distribution function

For a compact test set  $C \subset \mathbb{R}^d$ ,  $o \in C$ , the *contact distribution function* of a random closed set  $\Xi$  is introduced as

$$H_C(\rho) = P(d_C(o, \Xi) \leq \rho \mid o \notin \Xi), \quad \rho > 0,$$

where  $d_C(x, A) = \min\{\rho \geq 0 : (x + \rho C) \cap A \neq \emptyset\}$  is the distance from a point  $x \in \mathbb{R}^d$  to a closed set  $A \subset \mathbb{R}^d$  measured by “inflating” the test set  $C$ . It can be easily shown that

$$H_C(\rho) = P(\Xi \cap \rho C \neq \emptyset \mid o \notin \Xi) = \frac{T_\Xi(\rho C) - T_\Xi(\{o\})}{1 - T_\Xi(\{o\})},$$

cf. [20]. If  $\Xi$  is the Boolean model of Wiener sausages then  $T_\Xi(\{o\})$  is given by relation (3.8). The value of  $T_\Xi(\rho C)$  can be assessed numerically if  $C$  is a general compact set; see the next section for an example of such numerical analysis. However, if  $C$  is a unit ball then the *spherical contact distribution function*  $H_{B(o,1)}(\rho)$  can be given explicitly, since by (3.2) we get

$$T_\Xi(\rho B(o, 1)) = T_\Xi(B(o, \rho)) = 1 - e^{-\lambda \mathbb{E} V_d(S_{r,T} \oplus B(o, \rho))} = 1 - e^{-\lambda \mathbb{E} V_d(S_{r+\rho, T})}$$

which together with relation (3.6) yields the formula

$$H_{B(o,1)}(\rho) = 1 - e^{-\lambda M(d, \sigma^2, r, \rho, T)},$$

where

$$M(d, \sigma^2, r, \rho, T) = \omega_d ((r + \rho)^d - r^d) + \frac{d(d-2)}{2} \omega_d \sigma^2 ((r + \rho)^{d-2} - r^{d-2}) T + \frac{4d \omega_d}{\pi^2} \left( (r + \rho)^d \int_0^\infty \frac{1 - e^{-\frac{\sigma^2 y^2 T}{2(r+\rho)^2}}}{y^3 (J_\nu^2(y) + Y_\nu^2(y))} dy - r^d \int_0^\infty \frac{1 - e^{-\frac{\sigma^2 y^2 T}{2r^2}}}{y^3 (J_\nu^2(y) + Y_\nu^2(y))} dy \right).$$

### 3.3 Specific surface area

The specific surface area  $S_{\Xi}$  is defined as the mean surface area of  $\Xi$  per unit volume. More formally, consider the measure  $S_{\Xi}(B) = \mathbb{E} \mathcal{H}^{d-1}(\partial\Xi \cap B)$  for all Borel sets  $B \subset \mathbb{R}^d$ , where  $\mathcal{H}^{d-1}$  is the  $(d-1)$ -dimensional Hausdorff measure. Due to the stationarity of  $\Xi$ , the measure  $S_{\Xi}$  is translation invariant. By Haar's lemma, there exists a constant  $S_{\Xi} \in (0, \infty)$  such that  $S_{\Xi}(B) = S_{\Xi} \cdot V_d(B)$  for all Borel sets  $B$ . The factor  $S_{\Xi}$  is called the *specific surface area* of the Boolean model  $\Xi$  (cf. [20, p. 235]). The following formula (3.14) is well-known for Boolean models with compact grains; cf. Lemma 4.1 of [9].

**Proposition 3.1.** *The specific surface area of  $\Xi$  in  $\mathbb{R}^d$  ( $d = 2, 3$ ) is equal to*

$$S_{\Xi} = \lambda \mathbb{E} \mathcal{H}^{d-1}(\partial S_{r,T}) e^{-\lambda \mathbb{E} V_d(S_{r,T})}, \quad r > 0, \quad (3.14)$$

where the mean volume  $\mathbb{E} V_d(S_{r,T})$  is given in (3.6) and

$$\begin{aligned} \mathbb{E} \mathcal{H}^{d-1}(\partial S_{r,T}) &= d\omega_d r^{d-1} + \frac{4d^2 \omega_d r^{d-1}}{\pi^2} \int_0^\infty \frac{1 - e^{-\frac{\sigma^2 y^2 T}{2r^2}}}{y^3 (J_\nu^2(y) + Y_\nu^2(y))} dy \\ &\quad + d\omega_d \sigma^2 r^{d-3} T \left( \frac{(d-2)^2}{2} - \frac{4}{\pi^2} \int_0^\infty \frac{e^{-\frac{\sigma^2 y^2 T}{2r^2}}}{y (J_\nu^2(y) + Y_\nu^2(y))} dy \right) \end{aligned} \quad (3.15)$$

is the mean surface area of the Wiener sausage. In three dimensions, formula (3.14) simplifies to

$$S_{\Xi} = 2\pi\lambda \left( 2r^2 + 4r\sigma\sqrt{2T/\pi} + \sigma^2 T \right) e^{-2\pi\lambda r \left( 2/3r^2 + 2\sigma r\sqrt{2T/\pi} + \sigma^2 T \right)}. \quad (3.16)$$

## 4 Numerical assessment of the covariance function

As far as it is known to the authors, it is difficult to find an explicit analytical solution to (3.4) on the complement of the union of two spheres. Hence, numerical methods can be used to solve (3.4) and get a graph of the covariance function  $C_{\Xi}$ . In Section 4.1, we perform this numerical analysis by means of the finite element method (fem, for an introduction see [4, 5] and references quoted therein). Alternatively, a large number of Monte Carlo simulations of Wiener sausages can lead to precise estimates of  $C_{\Xi}$  as it is done in Section 4.3.

The MATLAB- and FEMLAB-Code which was used to compute the results below by the Monte-Carlo simulations resp. the finite element method can be downloaded from the web<sup>1</sup>.

<sup>1</sup><http://www.mathematik.uni-ulm.de/numerik/staff/funken/software>

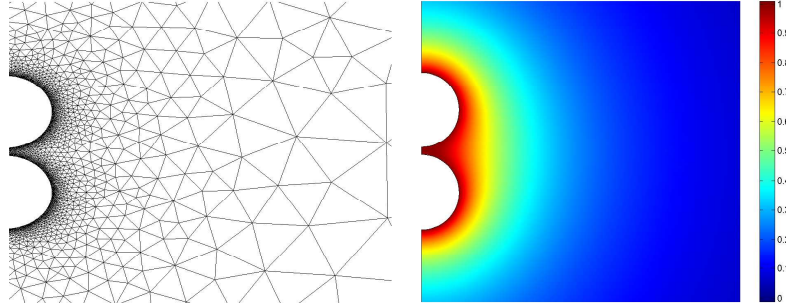


Figure 2: Zoom of the used fem mesh (left) and corresponding computed solution  $u$  (right) of (3.4) for  $d = 2$ ,  $\sigma = 1$ ,  $r = 1$ ,  $h = 2.2$  and  $t = 100$ .

#### 4.1 Numerical solution of the heat conduction problem

For  $d = 2, 3$  we used the finite element method to compute an approximate solution  $u$  of (3.4). To solve the problem efficiently we used rotational and axial symmetry in 3D resp. axial symmetries in 2D to reduce the complexity of problem (3.4). Furthermore, we restricted the resulting problem to a bounded domain  $\Omega_h$  with  $\max_{x,y \in \Omega_h} |x-y| > 10(2+h)$  for  $r = 1$ ,  $0 \leq h \leq 20$ , and  $0 \leq t \leq 100$ . This domain is large enough to provide the same numerical results for the problem (3.4), (3.12) solved in  $\Omega_h$ . For discretisation we used a graded mesh with minimal mesh size  $h_{\min} = 0.015$  along the boundary of the balls  $B(o, r)$ , resp.  $B(h \cdot u, r)$  and a mesh grading of 1.3, i.e. the rate how the mesh size grows as  $|x|$  tends to infinity. A zoom of the resulting finite element mesh is shown in Fig. 2 for  $r = 1$  and  $h = 2.2$ . As ansatzspace we used globally continuous, piecewise polynomials of degree 4 and an adaptive timestepping scheme. These calculations were done by using the software package FEMLAB/COMSOL [8] or can be done by adapting [1].

#### 4.2 Approximation formulae

In the following we shall give an approximation  $\tilde{C}_\Xi$  for the covariance function  $C_\Xi$  given in (3.9) for some fixed volume fraction  $p_\Xi$ , namely

$$C_\Xi(h) \approx \tilde{C}_\Xi(h) := 2p_\Xi - 1 + (1 - p_\Xi)^{\kappa(h,t)}, \quad (4.1)$$

with  $\kappa(h, t)$  given by (4.5), (4.6) below. Let  $d = 2, 3$  and

$$A_r(h, t) := \mathbb{E} V_d(S_{r,T} \cup (S_{r,T} + h \cdot u)) = V_d(B(o, r) \cup B(h \cdot u, r)) + \int_{\mathbb{R}^d \setminus (B(o,r) \cup B(h,r))} u(t, x) dx, \quad (4.2)$$

(compare (3.11)) where  $u(t, x)$  denotes the solution of (3.4) for some given  $h \geq 0$ ,  $r > 0$  and  $C \oplus B(r, o)$  as in (3.12). For some given volume fraction  $p_\Xi$

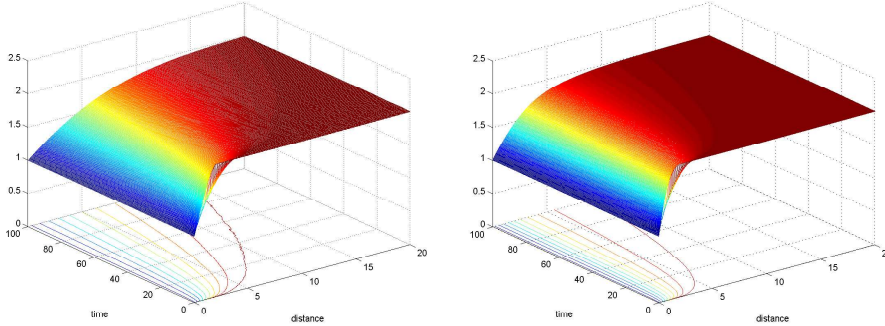


Figure 3: Computed approximation of  $A_r(h, t)/A_r(0, t)$  in 2D (left) resp. 3D (right) for  $r = 1$ ,  $0 \leq h \leq 20$  and total times  $0 \leq t \leq 100$ .

of the Boolean model  $\Xi$  we substitute  $\lambda$  implicitly defined by (3.8) in (3.10) which leads to

$$C_{\Xi}(h) = 2p_{\Xi} - 1 + (1 - p_{\Xi})^{A_r(h, t)/A_r(0, t)}.$$

For  $t = 0$  and  $d = 2$  analytic calculations of  $V_d(B(o, r) \cup B(h \cdot u, r))$  give

$$\frac{A_r(h, 0)}{A_r(0, 0)} = \kappa(h, 0) := \begin{cases} \frac{2}{\pi} \left( \pi - \arccos\left(\frac{h}{2r}\right) + \frac{h}{2r} \sqrt{1 - \left(\frac{h}{2r}\right)^2} \right), & \text{if } h \leq 2r, \\ 2, & \text{otherwise,} \end{cases} \quad (4.3)$$

resp. for  $d = 3$

$$\frac{A_r(h, 0)}{A_r(0, 0)} = \kappa(h, 0) := \begin{cases} \frac{1}{2} \left(\frac{h}{2r}\right)^3 - 2 \left(\frac{h}{2r}\right)^2 + \frac{5}{2} \frac{h}{2r} + 1, & \text{if } h \leq 2r, \\ 2, & \text{otherwise.} \end{cases} \quad (4.4)$$

For  $t > 0$  and  $d = 2, 3$  a closed formula for  $A_r(h, t)/A_r(0, t)$  is not known to the authors. In the following we give some approximation  $\kappa(h, \nu(t))$  (computed by the finite element method and some elementary postprocessing) to the quotient  $A_r(h, t)/A_r(0, t)$ , where we used the scaling invariants of  $A_r(h, t)/A_r(0, t)$  w.r.t. the radius  $r$ ,

$$\frac{A_r(h, t)}{A_r(0, t)} \approx \kappa(h, t) = \begin{cases} \left(\frac{h}{\nu(t)}\right)^3 - 3 \left(\frac{h}{\nu(t)}\right)^2 + 3 \frac{h}{\nu(t)} + 1, & \text{if } h \leq \nu(t), \\ 2, & \text{otherwise,} \end{cases} \quad (4.5)$$

with

$$\nu(t) = \begin{cases} 2.998 t^{0.3991} + 2.991, & d = 2, \\ 3.744 t^{0.2182} + 1.454, & d = 3. \end{cases} \quad (4.6)$$

Using (4.1) with (4.3) or (4.4) resp. (4.5) and (4.6) gives an approximation formula for the covariance function  $C_{\Xi}$ . For  $p_{\Xi} = 0.75$ ,  $r = 1$ ,

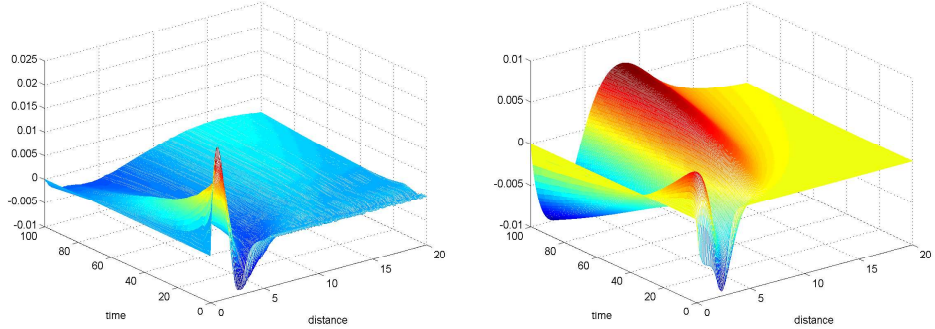


Figure 4: Estimated relative errors in 2D (left) resp. 3D (right) of covariance function  $|\overline{C}_{\Xi}(h) - \tilde{C}_{\Xi}(h)|/|\overline{C}_{\Xi}(h)|$  for  $p_{\Xi} = 0.75$ ,  $r = 1$ ,  $0 \leq h \leq 20$  and total times  $0 \leq t \leq 100$ .

$0 \leq h \leq 20$  and  $0 \leq t \leq 100$  numerical calculations show that point-wise in 2D the absolute error  $|\overline{C}_{\Xi}(h) - \tilde{C}_{\Xi}(h)| \leq 0.0134$ , the relative error  $|\overline{C}_{\Xi}(h) - \tilde{C}_{\Xi}(h)|/|\overline{C}_{\Xi}(h)| \leq 0.02$  resp. in 3D  $|\overline{C}_{\Xi}(h) - \tilde{C}_{\Xi}(h)| \leq 0.0063$  and  $|\overline{C}_{\Xi}(h) - \tilde{C}_{\Xi}(h)|/|\overline{C}_{\Xi}(h)| \leq 0.01$ , where  $\overline{C}_{\Xi}$  is the result of the computation of the covariance function by the finite element approximation.

### 4.3 Estimation by Monte–Carlo simulation

There are two ways leading to estimates of the covariance  $C_{\Xi}$  from simulations. The first way is to use the definition (3.9) and simulate many realizations of the Boolean model  $\Xi$  in a finite observation window estimating the two-point coverage probability from each of them and then averaging over all realizations. The second way is to simulate one Wiener sausage many times and estimate its covariogram. By expressions (3.10) and (3.13), this would lead to an estimate of the covariance  $C_{\Xi}$ . We would prefer the second approach since it leads to more precise results.

In order to do so, simulate  $N$  independent copies  $\{(S_{r,T,n})_k\}_{k=1}^N$  of the approximated Wiener sausage  $S_{r,T,n}$  for sufficiently large approximation parameter  $n$  and compute the volume of intersection  $S_{r,T,n} \cap (S_{r,T,n} + h \cdot u)$  by averaging over  $N$  realizations. To get a realization of  $S_{r,T,n}$ , we use a piecewise linear approximation  $W_i^n(t)$  of each coordinate  $W_i(t)$  of  $B(t) = B^o(t) = (W_1(t), \dots, W_d(t))$ , where  $W_i(t)$ ,  $i = 1, \dots, d$  are standard one–dimensional Wiener processes.

We assume for simplicity  $T = \sigma = 1$ . Let  $Y_0^i = 0$  and  $Y_1^i, Y_2^i, \dots$  be independent sequences of i.i.d. random variables with the distribution  $N(0, 1)$ ,  $i = 1, \dots, d$ . Set

$$S_n^i = \sum_{k=0}^n Y_k^i$$

to be a special case of the symmetric random walk. Introduce the piecewise linear process  $W_i^n(t)$ ,  $t \in [0, 1]$  by

$$W_i^n(t) = \frac{S_{k-1}^i}{\sqrt{n}} + \frac{nt - (k-1)}{\sqrt{n}} Y_k^i, \quad t \in \left[ \frac{k-1}{n}, \frac{k}{n} \right). \quad (4.7)$$

Following the well-known invariance principle of Donsker (cf. e.g. [3, Theorem 8.2]) it holds

$$W_i^n(t), t \in [0, 1] \xrightarrow{\mathcal{D}} W_i(t), t \in [0, 1], \quad n \rightarrow \infty, \quad i = 1, \dots, d. \quad (4.8)$$

In other words, the approximations  $W_i^n(t)$ ,  $i = 1, \dots, d$  converge in distribution to independent standard Wiener processes  $W_i$  on  $[0, 1]$ . It follows

$$B^n(t) = (W_1^n(t), \dots, W_d^n(t)), t \in [0, 1] \xrightarrow{\mathcal{D}} B(t), t \in [0, 1].$$

Set  $S_{r,1,n} = \{B^n(t) : t \in [0, 1]\} \oplus B(o, r)$  for any  $n \in \mathbb{N}$ . Let us show that the covariance function of the Boolean model with primary grain  $S_{r,1,n}$  approximates  $C_{\Xi}$  as  $n$  tends to infinity. It suffices to prove the following

**Proposition 4.1.** *It holds*

$$C_{S_{r,1,n}}(h) \rightarrow C_{S_{r,1}}(h), \quad n \rightarrow \infty, \quad h \geq 0. \quad (4.9)$$

First we need the following auxiliary result.

**Lemma 4.1.** *Let  $\{Y_i\}_{i \in \mathbb{N}}$  be a sequence of iid random variables with  $Y_i \sim N(0, 1)$ . Then, the inequality*

$$\mathbb{P} \left[ \max_{1 \leq k \leq n} |S_k| \geq x \right] \leq 2 \mathbb{P}[|S_n| \geq x/2], \quad x \geq 0$$

holds for  $S_k = Y_1 + \dots + Y_k$ ,  $k = 1, \dots, n$ .

*Proof.* Using arguments similar to [3, p. 256], one can prove the following variant of Etemadi's inequality:

$$\mathbb{P} \left[ \max_{1 \leq k \leq n} |S_k| \geq x \right] \leq \mathbb{P}[|S_n| \geq x/2] + \max_{1 \leq k \leq n} \mathbb{P}[|S_k| \geq x/2], \quad x \geq 0.$$

Since  $S_k \sim N(0, k)$ , it is easy to see that for any  $k = 1, \dots, n$

$$\mathbb{P}[|S_k| \geq y] = \frac{1}{\sqrt{2\pi}} \int_{\mathbb{R} \setminus (-y/\sqrt{k}, y/\sqrt{k})} e^{-z^2/2} dz \leq \mathbb{P}[|S_n| \geq y], \quad y \geq 0.$$

Hence, it holds

$$\max_{1 \leq k \leq n} \mathbb{P}[|S_k| \geq x/2] = \mathbb{P}[|S_n| \geq x/2],$$

and the lemma is proved.  $\square$

*Proof of Proposition 4.1.*

Since the mapping  $A \mapsto V_d(A \oplus B(o, r))$  is continuous in the Hausdorff metric (see the proof of [19, Theorem 3]), we have by the mapping theorem for convergence in distribution ([3, Theorem 2.7])

$$V_d(S_{r,1,n}) \xrightarrow{\mathcal{D}} V_d(S_{r,1}), \quad n \rightarrow \infty.$$

Our aim is to show that

$$\mathbb{E} V_d(S_{r,1,n}) \rightarrow \mathbb{E} V_d(S_{r,1}). \quad (4.10)$$

This convergence holds if  $V_d(S_{r,1,n})$ ,  $n = 1, 2, \dots$  are uniformly integrable random variables ([3, Theorem 3.5]). A sufficient condition for the uniform integrability is

$$\sup_{n \in \mathbb{N}} \mathbb{E}(V_d(S_{r,1,n}))^2 < \infty. \quad (4.11)$$

We can write

$$V_d(S_{r,1,n}) \leq \omega_d \left( r + \max_{t \in [0,1]} |B^n(t)| \right)^d \leq \omega_d \left( r + \sum_{i=1}^d \max_{t \in [0,1]} |W_i^n(t)| \right)^d.$$

Since the distributions of  $|W_i^n(t)|$ ,  $i = 1, \dots, d$  are identical we get

$$\begin{aligned} \mathbb{E}(V_d(S_{r,1,n}))^2 &\leq \omega_d^2 \mathbb{E} \left[ r + \sum_{i=1}^d \max_{1 \leq k \leq n} \frac{|S_k^i|}{\sqrt{n}} \right]^{2d} \\ &= \omega_d^2 \sum_{\substack{k_0, \dots, k_d \geq 0: \\ k_0 + \dots + k_d = 2d}} \frac{(d+1)!}{k_0! \dots k_d!} r^{k_0} \prod_{i=1}^d \mathbb{E} \max_{1 \leq k \leq n} \left( \frac{|S_k|}{\sqrt{n}} \right)^{k_i}, \end{aligned}$$

where  $S_k \stackrel{\mathcal{D}}{=} S_k^i \sim N(0, k)$ . Using Lemma 4.1, we get the upper bound

$$\begin{aligned} \mathbb{E} \max_{1 \leq k \leq n} \left( \frac{|S_k|}{\sqrt{n}} \right)^m &= \frac{1}{n^{m/2}} \int_0^\infty \mathbb{P} \left[ \max_{1 \leq k \leq n} |S_k| \geq x^{1/m} \right] dx \\ &\leq \frac{2}{n^{m/2}} \int_0^\infty \mathbb{P}[|S_n| \geq x^{1/m}/2] dx = \frac{2^{m+1}}{n^{m/2}} \int_0^\infty m y^{m-1} \mathbb{P}[|S_n| \geq y] dy \\ &= \frac{2^{m+1}}{n^{m/2}} \mathbb{E} |S_n|^m \leq m! 2^m, \quad m \in \mathbb{N}, \end{aligned}$$

where the latter inequality follows from the fact that  $S_n \sim N(0, n)$ . Hence, condition (4.11) is verified, and the convergence (4.10) of mean volumes holds.

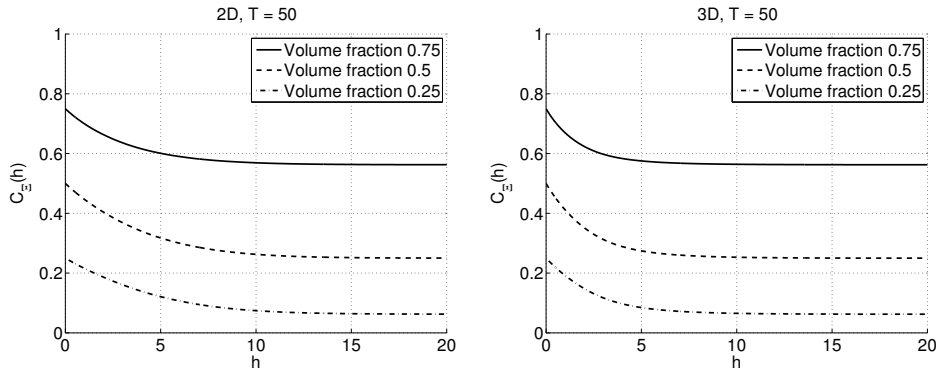


Figure 5: Estimated covariance functions of the planar and spatial Boolean model of Wiener sausages with  $r = 1$  and total time  $T = 50$ . In each case, the intensity  $\lambda$  is chosen to fit volume fractions 0.25, 0.5 and 0.75, respectively. Estimates for  $T = 1$  and  $T = 10$  are similar and therefore are omitted here.

We can proceed in the same way and show that

$$\begin{aligned} \mathbb{E} V_d(S_{r,1,n} + h \cdot u) &\rightarrow \mathbb{E} V_d(S_{r,1} + h \cdot u), \\ \mathbb{E} V_d(S_{r,1,n} \cup (S_{r,1,n} + h \cdot u)) &\rightarrow \mathbb{E} V_d(S_{r,1} \cup (S_{r,1} + h \cdot u)) \end{aligned}$$

as  $n \rightarrow \infty$ . Together with (3.11) we get relation (4.9), and Proposition 4.1 is proved. □

**Remark 4.1.** *According to the invariance principle of Donsker, Proposition 4.1 holds (with slight changes in the proof) for any choice of symmetric random walk  $S_n^i$  in (4.7). We choose the random variables  $Y_n^i$  standard normally distributed to reduce the error of approximation and increase the speed of convergence of the algorithm.*

Relation (4.9) together with the law of large numbers allow us to estimate the covariance function of the Boolean model  $\Xi$  from sufficiently many approximations  $S_{r,T,n}$ . In Figure 5, such estimates are given in two and three dimensions. For  $T = 1$ ,  $T = 10$  and  $T = 50$ , 10000 approximations of Wiener sausages with  $r = 1$  were simulated. To evaluate the volume of  $S_{r,T,n}$  and its covariogram numerically, realizations of Wiener sausages have to be discretized on a quadratic (cubic) grid in  $\mathbb{R}^2$  ( $\mathbb{R}^3$ ), and the number of pixels (voxels) belonging to  $S_{r,T,n}$  has to be counted. Hence, besides the error of the approximation of the Wiener sausage, the discretization error occurs.

	Monte–Carlo simulations		Finite element method	
	2D	3D	2D	3D
T=1	1 h 8 min	19 h 53 min	17.85 sec	19.15 sec
T=10	2 h 13 min	65 h 8 min	18.46 sec	19.45 sec
T=50	4 h 20 min	180 h 33 min	18.76 sec	20.06 sec

Table 1: Computing times for 1000 Monte–Carlo simulations and one finite element run to approximate the covariance function  $C_{\Xi}(h)$  for  $r = 1$  and total times  $T = 1$ ,  $T = 10$ , and  $T = 50$ .

Given the total runtime  $T$ , the maximal shift distance  $h_{max}$  for which the covariogram  $C_{S_r, T}$  was computed is given by

$$h_{max} = 2 \cdot F_{0, T}^{-1}(0.99),$$

where  $F_{0, T}^{-1}$  is the quantile function of the normal distribution  $N(0, T)$ . This value  $h_{max}$  yields a good empirical upper bound for the range of dependence of the covariance function  $C_{\Xi}$ . It means that  $C_{\Xi}(h) \approx p_{\Xi}^2$  is approximately constant for  $h > h_{max}$ .

#### 4.4 Comparison of results

We now compare the numerical calculations by the by the finite element method (Section 4.1) versus the Monte-Carlo simulation (Section 4.3) with respect to efficiency and accuracy.

Table 4.4 shows run times for both approaches to compute the covariance function  $C_{\Xi}(h)$  for  $r = 1$  and total times  $T = 1$ ,  $T = 10$ , and  $T = 50$  in two and three dimensions. Since adaptive time-stepping was used for the fem, the run time increases only slightly with increasing  $T$ . The run time of the Monte–Carlo method for  $T = 1$  corresponds roughly to 230 evaluations by the fem for different  $h$ . Due to rotational symmetry and the reduction of dimension, the run times for 2D and 3D using the fem are almost the same. In contrast, the Monte–Carlo simulations in 3D are much more time consuming. The run time depends on several factors such as efficiency of implementation, programming language, computer, to mention a few but not all; we believe, however, that the trend in Table 4.4 shows the overall efficiency of the fem.

In Figure 4.4 we depict the difference between the approximation of  $A_r(h, t)/A_r(0, t)$  by the finite element method and the Monte–Carlo simulations in 2D and 3D. Asymptotically both methods seem to converge to the same limit, namely 2. Preasymptotically the maximal difference for  $T = 10$  is less than 0.006 in 2D and less than 0.01 in 3D. Additional numerical experiments, where we decreased the mesh-size for the fem, did not give

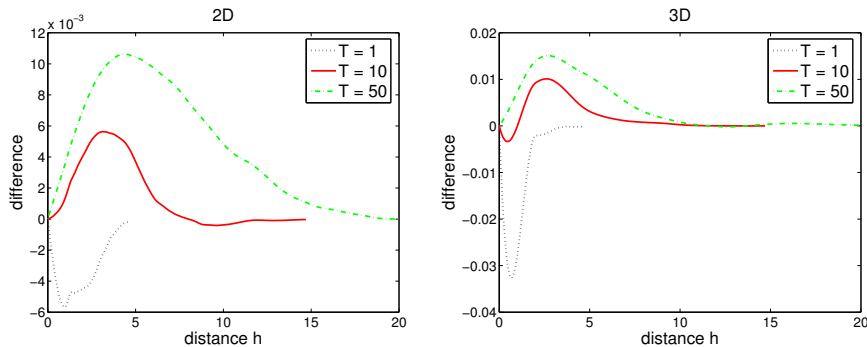


Figure 6: Differences in approximations of  $A_r(h, t)/A_r(0, t)$  by the finite element method (see Section 4.1) and the Monte–Carlo simulation (see Section 4.3) in 2D (left) resp. 3D (right) for  $r = 1$  and total times  $T = 1$ ,  $T = 10$  and  $T = 50$ .

smaller deviations which suggests that the fem is more accurate than the Monte–Carlo simulation.

To summarize, the comparison of the numerical performance of the finite elements method (fem) and the Monte–Carlo simulation shows clear advantages of the fem. Hence, fem can be recommended for the computation of the covariance function of the Boolean model of Wiener sausages.

## 5 Open problems

Beside the covariance function and the contact distribution function, there are many other quantities in stochastic geometry describing the geometrical properties of the Boolean model. As an example, *specific intrinsic volumes* (cf. e.g. [16]) can be mentioned including the volume fraction, the specific surface area and the specific Euler–Poincaré characteristic. They describe mean curvature properties of  $\Xi$ . Formulae for the volume fraction and the specific surface area are given in this paper. It is an open problem to find other  $d - 1$  specific intrinsic volumes of the Boolean model of Wiener sausages. The core of the problem lies in computing the mean curvature measures of the Wiener sausage explicitly. The first attempt to do that is made in the recent paper [13], where the computation of mean curvature measures is reduced to two *mean curvature functions* of Wiener paths. Unfortunately, the explicit form of these functions is still unknown.

## References

- [1] A. Albery, C. Carstensen, and S. Funken. Remarks around 50 lines of Matlab: short finite element implementation. *Num. Alg.*, 20:117–137, 1999.
- [2] A. M. Berezhkovskii, Yu. A. Makhnovskii, and R. A. Suris. Wiener sausage volume moments. *J. Stat. Phys.*, 57(1-2):333–346, 1989.
- [3] P. Billingsley. *Convergence of probability measures*. J. Wiley & Sons, New York, 1999.
- [4] D. Braess. *Finite Elements*. Cambridge University Press, 2001.
- [5] P.G. Ciarlet. *The Finite Element Method for Elliptic Problems*, volume 40 of *Classics in applied mathematics*. SIAM, 2002.
- [6] J. L. Doob. A probability approach to the heat equation. *Trans. Amer. Math. Soc.*, 80:216–280, 1955.
- [7] J.H.G. Fu. Tubular neighborhoods in Euclidean spaces. *Duke Math. J.*, 52:1025–1046, 1985.
- [8] S. Funken. Equation based modeling. *Simulation News Europe*, 37:11–14, 2003.
- [9] L. Heinrich and I. S. Molchanov. Central limit theorem for a class of random measures associated with germ–grain models. *Adv. Appl. Probab.*, 31:283–314, 1999.
- [10] G. A. Hunt. Some theorems concerning Brownian motion. *Trans. Amer. Math. Soc.*, 81:294–319, 1956.
- [11] G. Kesidis, T. Konstantopoulos, and S. Phoha. Surveillance coverage of sensor networks under a random mobility strategy. IEEE Sensors Conference, Toronto, October 2003. Proceedings paper.
- [12] A. Kolmogoroff and M. Leontowitsch. Zur Berechnung der mittleren Brownschen Fläche. *Physik. Z. Sowjetunion*, 4:1–13, 1933.
- [13] G. Last. On mean curvatures of Brownian paths. Preprint, Universität Karlsruhe, 2005. submitted.
- [14] G. Matheron. *Random Sets and Integral Geometry*. J. Wiley & Sons, New York, 1975.
- [15] I. S. Molchanov. *Statistics of the Boolean Model for Practitioners and Mathematicians*. J. Wiley & Sons, Chichester, 1997.

- [16] R. Schneider and W. Weil. *Stochastische Geometrie*. Teubner Skripten zur Mathematischen Stochastik. Teubner, Stuttgart, 2000.
- [17] S. Shakkottai. Asymptotics of query strategies over a sensor network. Preprint, 2004. To appear in the IEEE Transactions on Automatic Control, 2005.
- [18] F. Spitzer. Electrostatic capacity, heat flow, and Brownian motion. *Z. Wahrscheinlichkeitstheorie verw. Geb.*, 3:110–121, 1964.
- [19] L.L. Stachó. On the volume function of parallel sets. *Acta Sci. Math.*, 38:365–374, 1976.
- [20] D. Stoyan, W. S. Kendall, and J. Mecke. *Stochastic Geometry and its Applications*. J. Wiley & Sons, Chichester, 2nd edition, 1995.
- [21] A. S. Sznitman. Some bounds and limiting results for the measure of Wiener sausage of small radius associated with elliptic diffusions. *Stoch. Process. Appl.*, 25:1–25, 1987.
- [22] A.-S. Sznitman. *Brownian Motion, Obstacles and Random Media*. Springer, Berlin, 1998.
- [23] D.-Y. Yang, Yu. A. Makhnovskii, S.-Y. Sheu, and S. H. Lin. Simulation of the Wiener sausage. *Phys. Rev. E*, 62(3):3116–3120, 2000.

